

PERFORMANCE OF A CW-LASER REMOTE RAMAN SYSTEM. K. A. Horton, S. K. Sharma, N. Domergue-Schmidt, and P. G. Lucey, Hawaii Institute of Geophysics and Planetology, University of Hawaii, Honolulu, HI 96822 (keith@higp.hawaii.edu)

Introduction: Landers and rovers are an increasingly important element of NASA's solar system exploration program. Raman spectroscopy is typically envisioned as an *in situ* analysis technique. The potential for performing Raman analysis remotely has been explored theoretically [1] and experimentally [2]. Our concept of measuring Raman spectra remotely from a planetary lander [3] lends itself to combination with other techniques such as laser-induced breakdown spectroscopy (LIBS) [4] and atmospheric analysis with Raman lidar [5]. Remote liquid and gas detection by UV Raman spectroscopy has been shown to operate effectively over a range of 500 m to 1 km [6]. The results presented here demonstrate the ability to calibrate the intensity of the remote Raman signal.

Laboratory System: A laboratory version of the remote Raman spectroscopy system has been assembled consisting of: a Spectra Physics CW-laser operated at 488 nm, a CVI ¼-meter imaging spectrograph, a Photometrics CCD imager (1024x256 pixels) cooled to -105°C, a 4¼ inch, f/4.2 portable Newtonian telescope, and a data collection computer. An optical fiber bundle, which is formed into linear fiber array at the spectrograph, is used to connect the telescope to the spectrograph. The linear fiber array of thirty 50 µm fibers acts as the spectrograph slit, dispersing the received light across the entire CCD array. A holographic super-notch filter is adjusted to attenuate the elastically (Rayleigh) scattered and diffuse reflected laser light.

The laser and telescope are focused upon the same sample spot. Data are collected at distances of ~5 m and ~10 m from the telescope primary mirror. Combinations of laser power (at sample) and integration time have been investigated to derive a reasonable compromise of SNR and data acquisition efficiency.

Measurements: All measured samples are laid flat on a metal plate painted with spectrally-flat Krylon black paint positioned between 5-10 m from the telescope (controlled by the size of the lab). Powders are loosely packed in a metal cup also painted black and liquids are measured through a glass container placed on the black plate. The laser beam is redirected towards the sample using 3 first surface mirrors. The use of mirrors was necessary to minimize the angle between the incoming laser beam and the telescope's axis and to allow for vertical measurement of loose powders (or liquids). The laser beam diameter at 5.1 m is approximately 6 mm while the focused telescope spot size is 3 mm, thus the observed spot is overfilled.

Data Reduction and Calibration. Adapting common radiometric imaging techniques, all data are acquired in full-CCD image mode. This allows application of standard image processing methods to correct for array nonuniformity of offset and dark current (read-noise dominated), bad pixels, and cosmic ray hits. Bad pixels and cosmic rays are corrected by applying a local 5x5 median filter to each affected pixel. Flat-fielding of the image is accomplished by using a radiometrically calibrated source, a Labsphere integrating sphere, which corrects nonuniformity of array responsivity and also allows us to calibrate the observed signal to radiance. The final calibrated remote Raman spectrum in terms of scattering efficiency is then produced by averaging the entire image along the slit direction [7]. Wavelength calibration is achieved by performing a quadratic fit to the derived spectrum of a sample with well-known spectral peaks, usually calcite or Spectralon.

Where the sample fluorescence is significant, the background is removed from the spectrum automatically by evenly subsampling the spectrum by 20; applying a 3-element median filter to eliminate points falling on a peak; interpolating this sparse array back to the original spectrum length; subtracting the new smoothed array from the original spectrum, and adding back the minimum value to avoid applying an offset of the spectrum.

Results: Noise. A series of twenty sequential spectra were obtained on a sample of washed olivine grains in the size fraction range of 500-1000 µm. Data were acquired at a distance of 5.1 m, with an integration time of 60 s each, and at-target laser power of 250 mW. This olivine sample exhibited moderate fluorescence, which declined through the duration of the experiment. Figure 1 shows the resulting scattering efficiency spectra of the first and last of the twenty spectra collected, both exhibiting the characteristic Raman doublet near 850 cm⁻¹, but also evidencing a reduction in the fluorescence with exposure time. A plot of peak heights at 853 cm⁻¹ is shown in Figure 2. The plot indicates that the olivine underwent exponential quenching of the fluorescence. The lower curve in the plot shows the same peak heights after application of the automatic baseline removal. The slight negative slope of the straight-line fit is an artifact of the baseline removal algorithm.

Signal-to-Noise: The SNR for the olivine example just described was approximately 100. Because benzene is a well characterized strong Raman scatterer, we performed a series of measurements varying multiple parameters: distance to target (5m, 10 m); laser power (100, 150, 200, 250 mW); and integration time (30, 60,

180 s). Figure 3 shows the calculated SNRs at 5m and 10 m as a function of integration time for the 991 cm^{-1} peak. Figure 4 plots the best fit surface of SNR as a function of integration time and laser power.

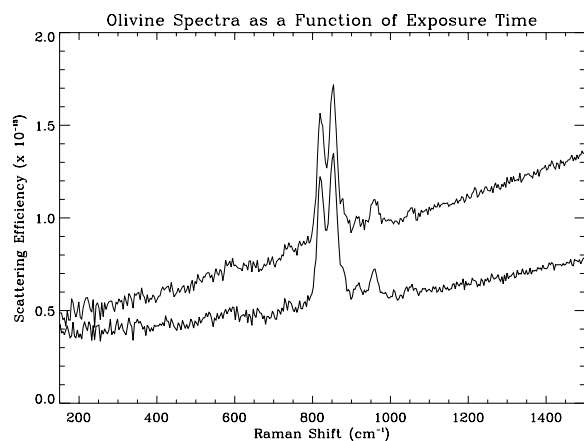


Figure 1. Spectra of olivine showing quenching of fluorescence after 20 subsequent exposures to laser excitation.

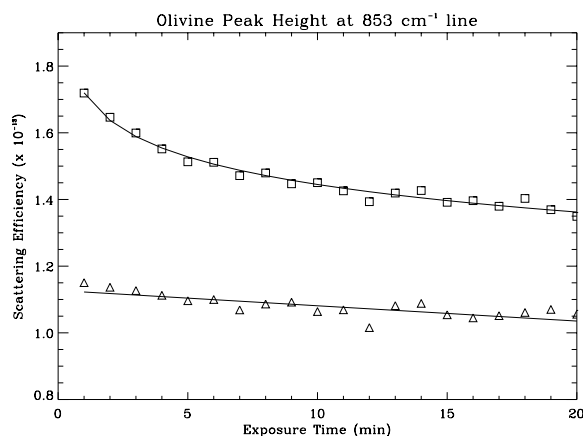


Figure 2. Effect of quenching on olivine peak height as a function of exposure time. Lower curve (triangles) has had automatic baseline removal applied; upper curve (squares) shows decrease of fluorescence with time.

Differential Cross Section: Knowledge of the beam dimensions and benzene volume sampled allowed us to calculate the differential scattering cross section of benzene. The following list compares our results to those previously published (normalized to 488 nm wavelength) and shows generally good agreement.

- This study: $[= 35.33 \pm 4.32 \times 10^{-30} \text{ cm}^2\text{sr}^{-1}$
 [8]: $[= 37.60 \pm 4.6 \times 10^{-30} \text{ cm}^2\text{sr}^{-1}$
 [9]: $[= 35.83 \pm 5.37 \times 10^{-30} \text{ cm}^2\text{sr}^{-1}$
 [10]: $[= 15.67 \times 10^{-30} \text{ cm}^2\text{sr}^{-1}$

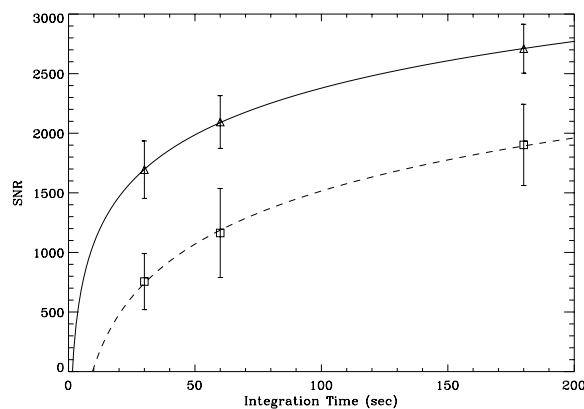


Figure 4. SNR of benzene at distances of 5m (solid) and 10m (dashed). Error bars give the RMS at 4 different excitation powers.

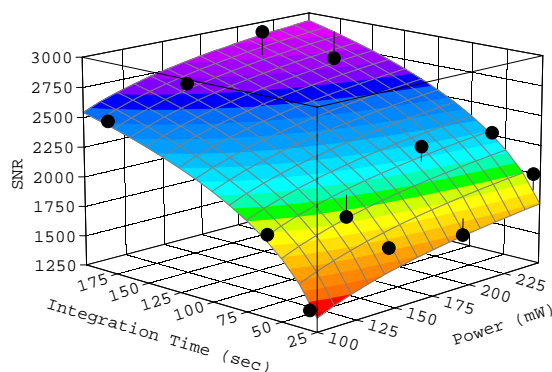


Figure 3. Best fit surface for SNR for benzene at 5m distance as a function of integration time and laser power.

As far as we are aware, this is the first report of cross sections derived from a sample at distance. The error reported includes data taken at different: distances, integration times, and different laser power levels.

References: [1] Hirschfeld (1974) *Appl. Optics*, 1435-1437. [2] Angel et al. (1992) *Appl. Spectrosc.*, 1085-1091. [3] Lucey, P.G. et al. (1998) *LPSC XXIX*, 1354-1355. [4] Wiens, R. C. et al. (2000) *LPSC XXXI*, #1468. [5] Sharma, S. K. et al. (2001) *LPSC XXXII*, this volume. [6] Wu, M. et al. (2000) *Appl. Spectrosc.* 54, 800-806. [7] Horton, K. A. et al. (2000) *LPSC XXXI*, #1514. [8] Eysel, H. et al. (1988) *J. Raman Spectrosc.* 59-64. [9] Ray, K. et al. (1997) *Appl. Spectrosc.*, 108-116. [10] Measures, R.M. (1984) Laser Remote Sensing, Fundamentals and Applications.